Great Framework Variation of Polymers in the Manganese(II) Maleate/α,α′-Diimine System: Syntheses, Structures, and Magneto-Structural Correlation

Chengbing Ma,[a,d] Changneng Chen,[a] Qiutian Liu,*[a] Feng Chen,[a] Daizheng Liao,[b] Licun Li,[b] and Licheng Sun[c]

Keywords: Crystal structure / Maleic acid / Magnetic properties / Manganese / Structural topology

Three novel manganese(II) coordination polymers, $[Mn(maleate)(phen)]_n$ (**1**; phen = 1,10-phenanthroline), $[Mn(maleate)(phen)]_n \cdot nH_2O$ (**2**), and $[Mn(maleate)(bpy)]_n$ (**3**; bpy = 2,2′-bipyridine), have been synthesized by treatment of Mn^{2+} with maleic acid with participation of chelate diimine ligands, and have been identified by single-crystal X-ray diffraction to have either one-dimensional (1D) zigzag chain structures (**1** and **2**) or a two-dimensional (2D) sinuous layer structure (**3**). Each maleate dianion coordinates to three Mn centers, in different bridging modes (*syn-anti* in **1** and **2**, *syn-syn* and *anti-anti* in **3**). These compounds represent an interesting example of structural topology variation from 1D to 2D mediated by chemically similar auxiliary chelate ligands. Variable-temperature magnetic susceptibility measurements show weak anti-ferromagnetic exchange interactions between the adjacent Mn^{II} ions, with $J = -0.06$ cm^{-1} (**2**) and $J = -1.3$ cm^{-1}, $zJ' = -0.27$ cm^{-1} (**3**). The differences in the magnitudes of these coupling interactions agree well with the nature of the carboxylate-bridging coordination of maleate.

Introduction

There is currently great interest in the construction of metal-organic hybrid extended solids containing paramagnetic metal ions, driven to a large extent by their fascinating network topologies and their wide applications, such as in the field of molecular magnetism.[1] The key to the fabrication of such networks is the selection of appropriate bridging ligands capable of mediating magnetic interaction and coordination geometries of metal ions.[2] The recent exponential growth in the synthesis and study of such coordination polymers has provided elegant examples of how the metal ion geometry and the appropriate bridging ligand symmetry can be exploited for the design of materials with unusual structures and properties. In this respect, polycarboxylate ligands are frequently used as magnetic superexchange pathways between the metal ions, due to their versatile carboxylate-bridging coordination modes (*syn-syn*, *anti-anti*, and *syn-anti*) capable of transmitting magnetic coupling interactions to different degrees.[3]

The product architecture that will spontaneously self-assemble from a metal node and a single organic spacer can to some extent be predicted in the light of the known metal coordination preference and the ligand configuration.[4] The introduction of another ligand, however, will greatly reduce the reliability of the prediction. In this situation, the auxiliary ligand may affect the combination mode of the metal ion with a primary ligand, finally resulting in topologically different complexes.

In the course of our study on manganese complexation by polyacids, we pay special attention to the influence of auxiliary ligands on the structural topology,[5] since at present it is not possible to know for certain the differences between the compounds.[6] In this work, we selected maleate as a primary ligand, in view both of its versatile bonding modes, capable of linking more than one metal ion, and also of its specific conformation, which was predicted to yield extended structures. We obtained two types of manganese(II) polymers with 1D and 2D frameworks in the presence of phen and bpy, respectively, as the secondary ligands. The result shows profound influences of the auxiliary chelate ligand both on the structural topology and on the simultaneous adoption of maleate coordination modes (Scheme 1), followed accordingly by the alteration of the magnetic properties of the product.

[a] State Key Laboratory of Structural Chemistry, Fujian Institute of Research on the Structure of Matter, Chinese Academy of Sciences,
Fuzhou 350002, China
Fax: (internat.) + 86-591/3714946
E-mail: lqt@ms.fjirsm.ac.cn
[b] Department of Chemistry, Nankai University,
Tianjin 300071, China
[c] State Key Laboratory of Fine Chemicals, Dalian University of Technology,
Dalian, China
[d] Graduate School of the Chinese Academy of Sciences,
Beijing, China

  DOI: 10.1002/ejic.200300097

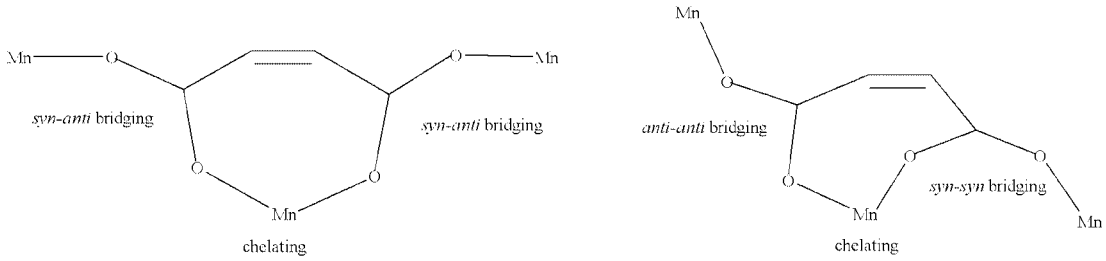

Scheme 1. A schematic illustration showing the coordination modes of maleate dianion observed in complexes **1**−**3** (left for **1** and **2**, right for **3**)

Results and Discussion

Synthesis

Three polymers were produced from the Mn^{2+}/maleate/diimine self-assembly system. Although structurally unexpected complexes are frequently encountered, as the metal−ligand self-assembly is strongly influenced by factors such as the solvent system, template, and counter-ion, as well as the preferences of metal center and organic spacer conformation, the dramatic difference derived from chemically very similar ancillary ligands, such as observed in the present work, is rather surprising. Attempts to obtain a complex topologically similar to **3** with bpy instead of phen under various reaction conditions did not succeed, and vice versa. The production of great structural variation, from 1D to 2D, for the two types of polymers (vide supra) may be due to the difference in conjugate ring area in the auxiliary ligands bpy and phen.

Structure Descriptions of Complexes 1−3

Single-crystal X-ray diffraction analysis reveals that the complex **1** is a 1D, neutral, chain-like polymer consisting of [Mn(maleate)(phen)] units. The Mn^{II} center has a distorted octahedral geometry with four O atoms of three maleate ligands [Mn−O 2.117(2)−2.208(2) Å] and two N atoms of one phen ligand [Mn−N 2.334(2) and 2.308(2) Å] at the six corners. Selected bond lengths and angles are listed in Table 1. Each Mn ion is coordinated by three maleate ions, while each maleate coordinates to three Mn ions through its two carboxylate groups in chelating and bridging modes. Two oxygen atoms of the two ends of the maleate ion chelate one Mn atom to form a seven-membered ring (**A**); meanwhile, each of the carboxylate groups bridges two Mn atoms in a *syn-anti* fashion, resulting in double μ-OCO bridges and a bridging eight-membered ring (**B**), as shown in Figure 1. Consequently, these different non-planar **A** and **B** rings alternately interlock by sharing the C−O−Mn edges to produce a one-dimensional zigzag chain (Figure 2), in which every two neighboring symmetry-related Mn atoms are separated by 4.976 Å. In addition, there is a significant π−π-stacking interaction between the phen ligands belonging to the inversion-related chains ($-x$, $1 - y$, $1 - z$) with a perpendicular ring separation of 3.363 Å, which further promotes the stabilization of the zigzag chain.

Complex **2** is made up of a one-dimensional chain and solvate water molecules. The chain is constructed from basic [Mn(maleate)(phen)] units, the structures of which are almost identical to those in **1**, and all the structural parameters are also very close to those of **1**, as can be seen from Table 1. Two hydrogen bonds link the lattice water molecule

Table 1. Selected bond lengths [Å] and angles [°] of **1** and **2** (symmetry transformations used to generate equivalent atoms: A: $-x$, $-y + 1$, $-z + 2$; B: $-x + 1$, $-y + 1$, $-z + 2$; C: $-x + 1$, $-y + 2$, $-z$; D: $-x$, $-y + 2$, $-z$)

Complex **1**							
Mn−O1	2.117(2)	Mn−O4B	2.123(2)	Mn−O2A	2.176(2)	Mn−O3	2.208(2)
Mn−N2	2.308(2)	Mn−N1	2.334(2)	O1−Mn−O4B	101.70(8)	O1−Mn−O2A	93.26(7)
O4B−Mn−O2A	89.63(7)	O1−Mn−O3	84.92(7)	O4B−Mn−O3	89.97(8)	O2A−Mn−O3	178.02(7)
O1−Mn−N2	170.56(8)	O4B−Mn−N2	87.72(8)	O2A−Mn−N2	86.11(7)	O3−Mn−N2	95.81(7)
O1−Mn−N1	98.84(8)	O4B−Mn−N1	159.14(9)	O2A−Mn−N1	92.82(8)	O3−Mn−N1	88.24(8)
N2−Mn−N1	71.80(8)						
Complex **2**							
Mn−O1	2.124(3)	Mn−O4C	2.156(3)	Mn−O2D	2.193(3)	Mn−O3	2.198(3)
Mn−N2	2.286(3)	Mn−N1	2.320(4)	O1−Mn−O4C	100.62(12)	O1−Mn−O2D	94.35(11)
O4C−Mn−O2D	86.82(11)	O1−Mn−O3	85.00(11)	O4C−Mn−O3	88.27(12)	O2D−Mn−O3	174.85(11)
O1−Mn−N2	169.65(12)	O4C−Mn−N2	89.69(13)	O2D−Mn−N2	87.02(11)	O3−Mn−N2	94.53(11)
O1−Mn−N1	97.42(12)	O4C−Mn−N1	161.8 (1)	O2D−Mn−N1	93.99(12)	O3−Mn−N1	91.16(12)
N2−Mn−N1	72.25(13)						

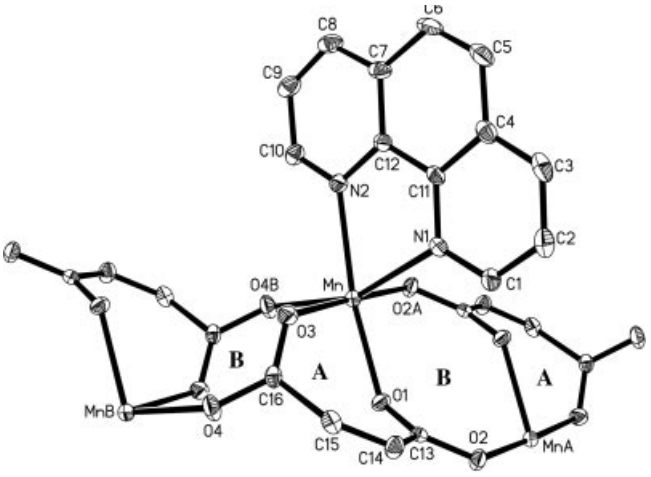

Figure 1. Structure view of **1** showing the local coordination environment of Mn^{II} with thermal ellipsoids at 30% probability (**A** and **B** represent two kinds of microcycles)

O5 and two carboxylate oxygen atoms of symmetry-related polymer chains to generate a two-dimensional network sheet (Figure 3).

Interestingly, the replacement of phen by bpy resulted in the crystallization of the architecturally significantly different complex **3**, the structure of which involves a two-dimensional layer framework composed of neutral [Mn(maleate)(bpy)] units. Selected bond lengths and angles are listed in Table 2. Each Mn^{II} ion completes its pseudoctahedral geometry with four oxygen atoms of three maleate ions and two nitrogen atoms of a chelating bpy ligand (Figure 4). Each maleate ligand is also bonded to three different Mn atoms in chelating and bridging modes, and the chelating mode results in a seven-membered ring **A**, like those in **1**. Two carboxylate groups act as triatomic bridges in two distinct bridging modes (*syn-syn* and *anti-anti*), which are greatly different from that found in **1** (*syn-anti*). The *syn-syn* bridge forms an eight-membered ring $Mn_2(\mu\text{-}OCO)_2$ unit (**B**), which is fused together with two **A** rings by shar-

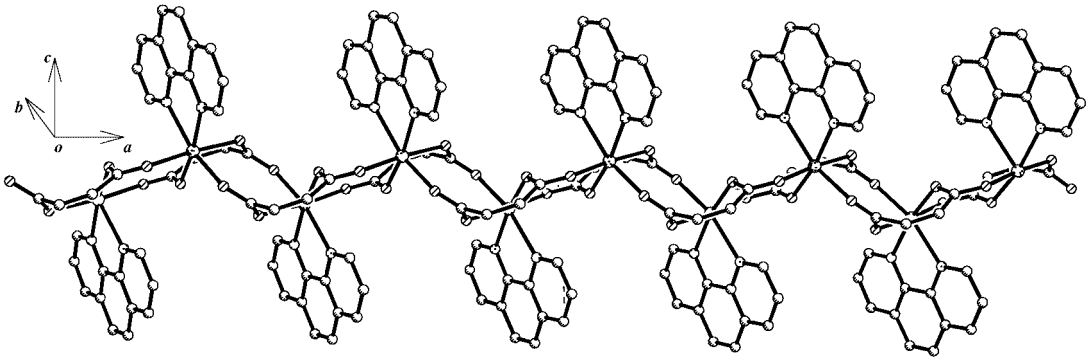

Figure 2. A view of the 1D zigzag chain in **1**, with hydrogen atoms omitted for clarity

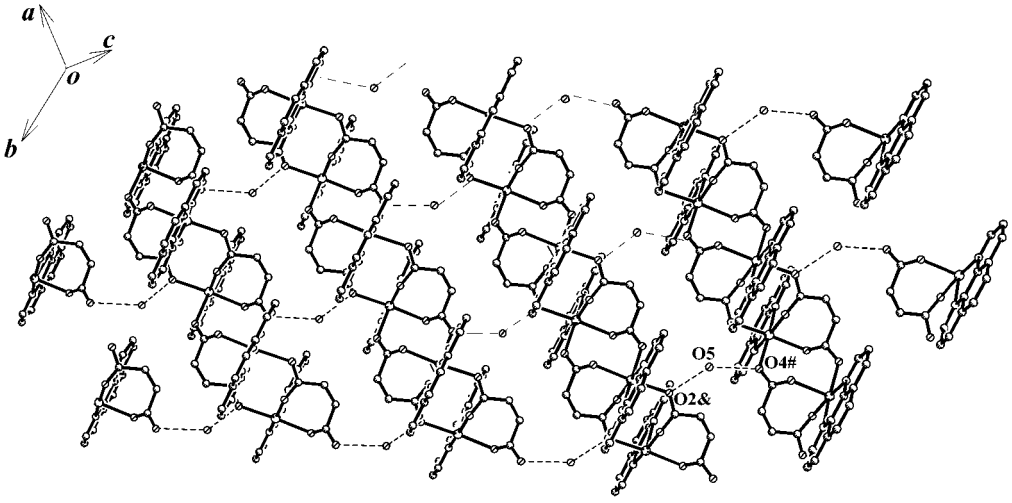

Figure 3. A packing diagram showing part of the two-dimensional hydrogen-bonded network (O5−H5B···O4# = 3.006 Å and O5−H5C···O2& = 2.943 Å); symmetric modes: #: $x - 1, y - 1, z$; &: $-x, -y + 2, -z$

ing Mn−O−C edges to form **ABA** fused rings. The *anti-anti* bridge bridges between the two **ABA** moieties, resulting in a 22-membered macrocycle **C**, containing four Mn atoms alternately linked by four maleate ligands. The *syn-syn* and *anti-anti* bridges give rise to two spans with Mn−MnA distances of 4.666 Å and Mn−MnB distances of 6.390 Å, respectively. These rings extend sequentially to build up a two-dimensional sinuous layer-type architecture (Figures 5 and 6) with bpy ligands protruding towards the interlayer region, as shown in Figure 6. It is indicated that the **ABA-BAB**... zigzag chain of **1** arises from the mutual interlock of the **A** and **B** rings, while the linkage of the **ABA** moieties through the carboxylate group bridge gives rise to the clearly different framework topology of **3**. Surprisingly, this dramatic difference between the two complexes actually derives from chemically very similar ancillary ligands, phen and bpy. It is believed that the larger ring area of the phen ligand may be preferable for production of π−π interactions (vide supra) between the aromatic rings, albeit weak. This would favor the formation of a zigzag chain. However the larger ring area may also produce a spatial hindrance

Table 2. Selected bond lengths [Å] and angles [°] of complex **3** (symmetry codes: A: $-x + 1, -y + 1, -z$; B: $x, -y + 3/2, z + 1/2$)

Mn−O1	2.1156(18)	Mn−O4B	2.151(2)
Mn−N1	2.273(2)	Mn−N2	2.333(2)
Mn−O2A	2.1744(19)	Mn−O3	2.1821(2)
O1−Mn−O4B	99.55(8)	O1−Mn−O2A	94.64(7)
O4B−Mn−O2A	84.29(8)	O1−Mn−O3	82.92(7)
O4B−Mn−O3	94.08(8)	O2A−Mn−O3	176.81(8)
O1−Mn−N1	166.47(8)	O4B−Mn−N1	89.84(8)
O2A−Mn−N1	95.98(8)	O3−Mn−N1	86.74(8)
O1−Mn−N2	100.52(8)	O4B−Mn−N2	159.25(8)
O2A−Mn−N2	88.89(8)	O3−Mn−N2	93.56(8)
N1−Mn−N2	71.36(8)		

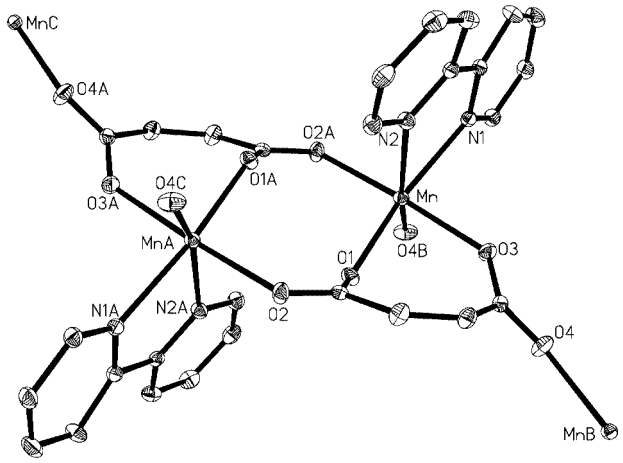

Figure 4. Structure view of **3** showing the local coordination environment of Mn^{II} with thermal ellipsoids at 30% probability

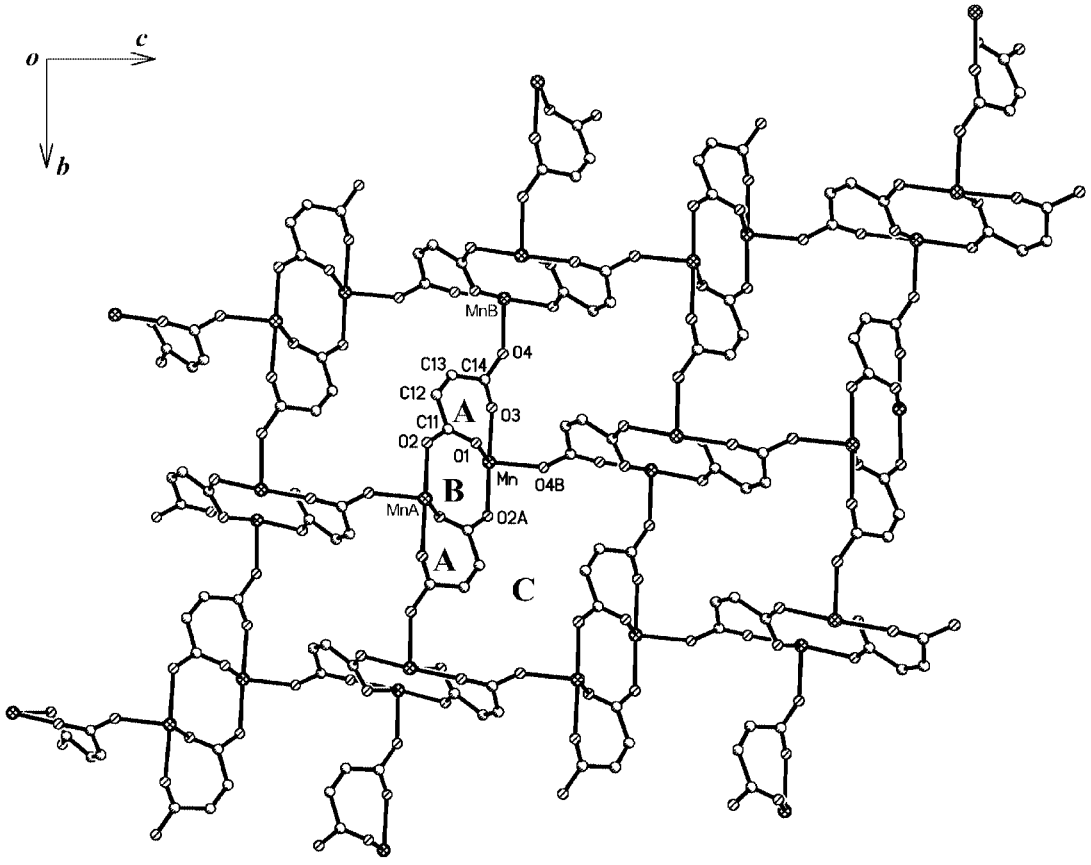

Figure 5. A view of the layer structure of **3**, with hydrogen atoms and bpy ligands omitted for clarity (**A**, **B**, and **C** represent three different subrings)

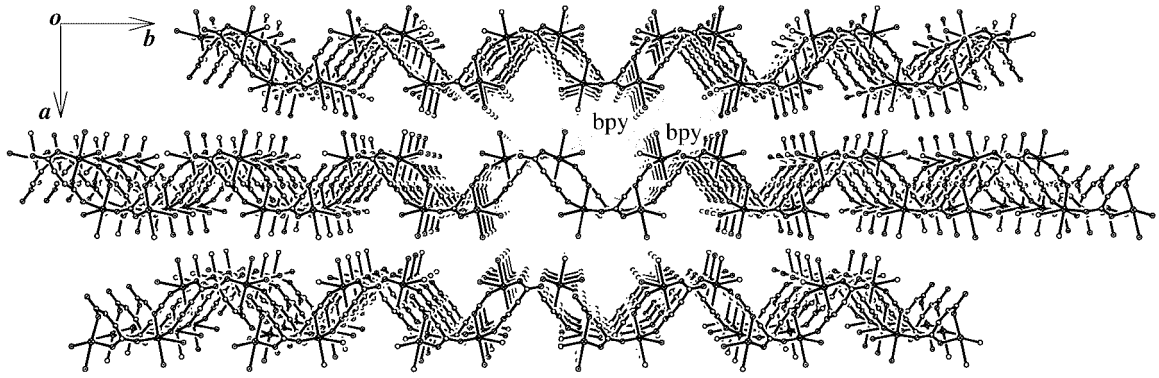

Figure 6. The packing diagram of **3** focused on the sinusoid-like layer framework; carbon atoms of bpy ligands are excluded for clarity

between the two sinuous layers (Figure 6). Consequently, the participation of the two ancillary ligands results in different framework topologies.

To the best of our knowledge, the coordination mode of maleate in **1**−**3** is unique in metal maleate/diimine systems, and different from that found in a tetramanganese cluster $[Mn_4(maleate)_2(bpy)_8](ClO_4)_4$,[7] in which each maleate ligand carboxylate group bridges two manganese ions in an *anti-anti* fashion, and also from that found in a manganese polymer $[Mn(maleate)(L)]_n$ (L = 4,4′-bipyridine),[8] in which two carboxylate groups of the maleate ligand act as a triatomic bridge in a *syn-anti* fashion and a monoatomic bridge to link two manganese ions, respectively, with the fourth carboxylate oxygen atom free. In addition, there were three previously reported dinuclear Cu/Zn maleate/bpy (or phen) complexes[9] in which the metal ions are five-coordinate and the maleate ion serves as a bidentate ligand linking two metal ions through two oxygen atoms of its two ends, and one mononuclear complex $[Co(maleate)(bpy)(H_2O)_3]\cdot H_2O$,[10] in which the maleate ion binds to the six-coordinate Co center through only one carboxylate oxygen atom. No other metal maleate/α-α′-diimine polymeric complexes have been reported so far.

IR Spectroscopy

The IR spectra of the three complexes clearly show both the presence of the maleate ion and its coordination mode. The strong absorptions at 1560 and 1425 cm^{-1} for **1**, 1558 and 1427 cm^{-1} for **2**, and 1551 and 1429 cm^{-1} for **3** correspond to asymmetric and symmetrical stretching vibrations − $\nu_{as}(COO)$ and $\nu_s(COO)$, respectively − of the coordinated carboxylate groups. The differences ($\Delta = \nu_{as} - \nu_s$) between $\nu_{as}(COO)$ and $\nu_s(COO)$ (135 cm^{-1} for **1**, 131 cm^{-1} for **2**, and 122 cm^{-1} for **3**) are significantly smaller than the corresponding value of 200 cm^{-1} for the free maleate dianions,[11] indicating a bidentate bridging coordination mode of the carboxylate groups.[12] This is in accordance with the result of X-ray diffraction analysis. In addition, the strong and broad band centered at 3450 cm^{-1} for **2** is attributable to the H−O−H stretching vibration of the lattice water molecule on the basis of the known structure. The medium absorptions at 3051 cm^{-1} for **1**, 3053 cm^{-1} for **2**, and 3046 cm^{-1} for **3** can be attributed to δ(=C−H) of maleate.

Magnetic Properties

Variable-temperature magnetic susceptibility measurements in the 5−300 K range were carried out for complexes **2** and **3**, and are shown in Figure 7. For **2**, the effective experimental magnetic moment (μ_{eff}) per Mn^{II} ion at room temperature is 5.70 μ_B, slightly lower than that of the uncoupled Mn^{2+} ion ($S = 5/2$; 5.91μ_B), remaining practically constant down to 30 K, and then gradually decreasing with decreasing temperature, reaching a value of 5.20 μ_B at 5 K. The $1/\chi_M$ vs. T plot is essentially linear (see inset in Figure 7), and obeys the Curie−Weiss law [$\chi_M = C/(T - \theta)$] with $C = 4.0\ cm^3\cdot K^{-1}\cdot mol$ and $\theta = -0.85$ K. In view of the known structure of the complex, the experimentally determined magnetic behavior was fitted by use of Equation (1) according to an isotropic Heisenberg model for a linear chain of metal ions with coefficients generated by Hiller et al.[13] for $S = 5/2$, where $A = 2.9167$, $B = 208.04$, $C = 15.543$, $D = 2707.2$, and $X = J/kT$. The best fitting parameters obtained are $J = -0.06\ cm^{-1}$, $g = 1.96$, with an agreement factor $R = 4.00\cdot10^{-4}$. This very small J value indicates very weak coupling interactions between the metal ions mediated by a triatomic *syn-anti* carboxylate group bridge, or practically a non-coupled system.

$$\chi_M = \left(Ng^2\beta^2/kT\right)(A + BX^2)(1 + CX + DX^3)^{-1} \quad (1)$$

For **3**, the experimentally determined effective magnetic moment at room temperature is 5.89 μ_B per Mn^{II} ion, very close to that of a magnetically isolated Mn^{2+} ion ($S = 5/2$; 5.91 μ_B). Upon cooling, the value decreases continuously down to 2.95 μ_B at 5 K, indicating an overall antiferromagnetic coupling interaction between the metal ions. From the known structural data, there are two types of magnetic exchange pathways between adjacent Mn^{2+} centers: one occurs between two doubly carboxylate-bridged (*syn-syn*

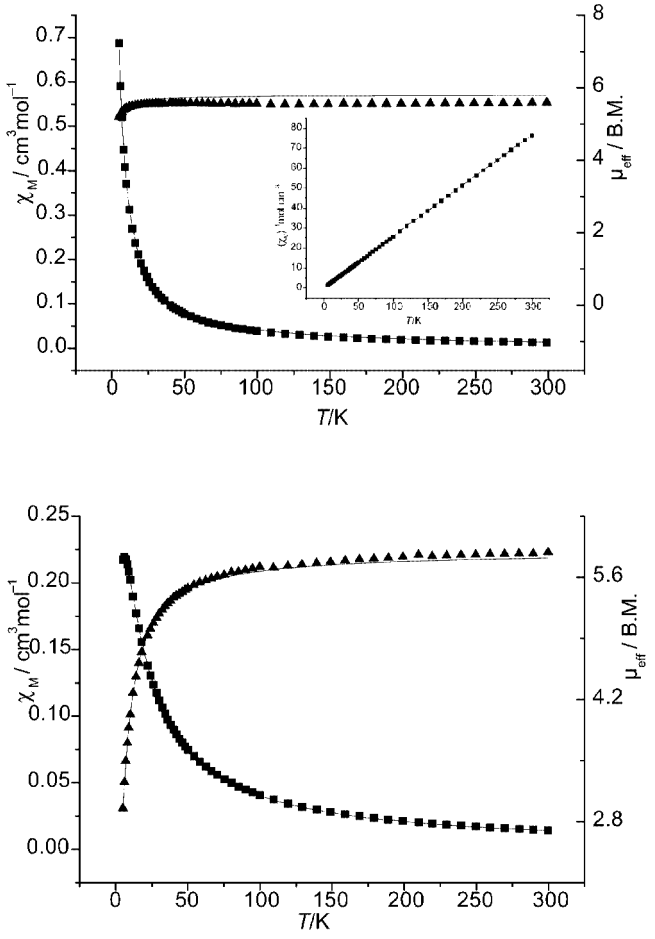

Figure 7. Experimental susceptibilities (χ_M, marked as square) and effective magnetic moment (μ_{eff}, marked as triangle) as functions of the temperature for complex **2** (top) and **3** (bottom); the solid lines represent the calculated values

mode) Mn^{2+} ions, and the other between singly carboxylate-bridged (*anti-anti* mode) Mn^{2+} ions. In view of the long separation (6.390 Å) of the *anti-anti*-bridged Mn^{2+} ions, we can simplify the coupling interaction system as a dimanganese(II) moiety, and simulate the magnetic behavior by use of Equation (2)[14] deduced from the Hamiltonian $\hat{H} = -J\hat{S}_1 \cdot \hat{S}_2$.

$$\chi_{bi} = \frac{2Ng^2\beta^2}{kT}\left[\frac{55+30\exp\left(-\frac{5J}{kT}\right)+14\exp\left(-\frac{9J}{kT}\right)+5\exp\left(-\frac{12J}{kT}\right)+\exp\left(-\frac{14J}{kT}\right)}{11+9\exp\left(-\frac{5J}{kT}\right)+7\exp\left(-\frac{9J}{kT}\right)+5\exp\left(-\frac{12J}{kT}\right)+\exp\left(-\frac{14J}{kT}\right)}\right] \quad (2)$$

To improve on the calculated expression, a mean molecular field approximation term[15] zJ' was added to describe the inter-dimer Mn^{2+} unit exchange interactions. The expression for the magnetic susceptibility becomes $\chi_M = \chi_{bi}/(1 - zJ' \cdot \chi_{bi}/Ng^2\beta^2)$. A satisfactory fitting result with parameters $J = -1.3$ cm^{-1}, $zJ' = -0.27$ cm^{-1}, $g = 1.99$, and the agreement factor $R = 3.25 \cdot 10^{-5}$ was obtained over the full temperature range.

All magnetic coupling interaction parameter values (J and zJ') fall in the normal range for two adjacent Mn^{2+} ions through the carboxylate group pathway, and the difference in the magnitude of the magnetic coupling interactions found for **2** and **3** can be explained in terms of the bridging modes of the carboxylate group and the overlap of d-p magnetic orbitals. As would be expected on the basis of the respective geometries, there is an efficient overlap between the 3d magnetic orbital of the Mn^{2+} center and the 2p magnetic orbital of the carboxylate group O in the order *syn-syn* > *anti-anti* > *syn-anti* (Scheme 2).[16] In good agreement with this, despite the larger separation of Mn···Mn (6.390 Å) in **3** than in **2** (4.976 Å), the corresponding exchange interaction value $zJ' = -0.27$ cm^{-1} in the *anti-anti* mode is larger than that of the *syn-anti* mode ($J = -0.06$ cm^{-1}, so small that the interaction is actually negligible) for **2**. Also, the *syn-syn* mode in complex **3** results in the largest J value, showing that the *syn-syn* carboxylate group bridge is more favorable than the others for transmission of the magnetic coupling interaction.[17]

Conclusion

We have obtained three novel manganese(II) polymeric complexes **1**, **2**, and **3**, variously possessing 1D zigzag chain and 2D sinuous layer structures, based on maleic acid in the presence of ancillary α,α′-diimine ligands (1,10-phenanroline and 2,2′-bipyridine). Very similar ancillary chelate ligands result in different structural topologies, which may be attributable to the different ring areas of the two delocalized aromatic diimine ligands, suggesting that the polymeric coordination framework may be designed and synthesized according to the inherent steric constraint and interactive information stored in organic ligands and metal ions,[4a,18] or modified through appropriate ancillary ligands. Studies on the magnetic properties of the complexes revealed weak antiferromagnetic coupling interactions between the paramagnetic Mn^{II} sites mediated to different degrees by the carboxylate group bridges in *syn-syn*, *anti-anti*,

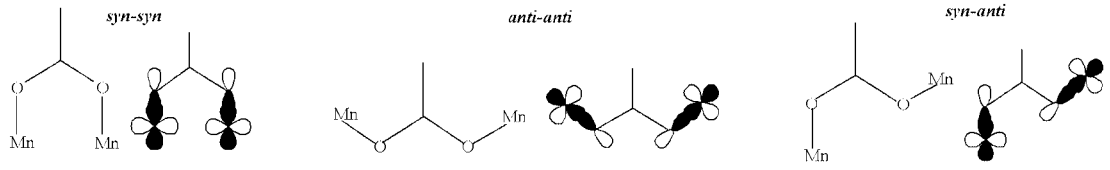

Scheme 2. Schematic representations of the coordination modes for the triatomic carboxylate bridge and the overlap of d-p magnetic orbitals

and *syn-anti* modes. The magnitudes of the *J* values for the interactions can be explained in terms of the efficient overlap between the magnetic orbitals. Various bridging modes of the carboxylate groups give the order *J* (*syn-syn*) > *J* (*anti-anti*) > *J* (*syn-anti*) for the interactions.

Experimental Section

General: All chemicals were of reagent grade and were used as received. Elemental analyses were performed with a Vario EL III CHNOS element analyzer, and the metal analysis was carried out by standard EDTA titration methods. IR spectra of KBr pellets (4000−400 cm^{-1}) were recorded with a Magna-75-FT-IR spectrophotometer.Variable-temperature susceptibility was measured with a model CF-1 superconducting magnetometer with a crystalline sample kept in a capsule at 4.5−300 K. Diamagnetic corrections were made with Pascal's constants for all the constituent atoms of the determined complexes.

Synthesis of [[Mn($C_4H_2O_4$)($C_{12}H_8N_2$)]$_n$ (1): A solution of 1,10-phenanthroline (0.20 g, 1 mmol) in ethanol (10 mL) was added to a suspension of $MnCO_3$ (0.12 g, 1 mmol) and maleic acid (0.17 g, 1 mmol) in water (20 mL). The mixture was heated at reflux for 8 d, during which yellow crystals were produced. These were collected to afford **1** (0.08 g, yield 22.6% based on Mn). $C_{16}H_{10}MnN_2O_4$ (349.20): calcd. C 55.03, H 2.89, Mn 15.73, N 8.02; found C 54.76, H 3.07, Mn 15.98, N 8.11. IR: $\tilde{\nu}$ = 3051 (m), 1633 (m), 1620 (s), 1560 (vs), 1514 (m), 1425 (s), 1402 (w), 1346 (w), 1309 (vs), 1200 (w), 1144 (w), 1101 (w), 1088 (w), 889 (m), 850 (s), 783 (m), 731 (s), 661 (w), 634 (w), 619 (m), 550 (m), 418 (m) cm^{-1}.

Synthesis of [Mn($C_4H_2O_4$)($C_{12}H_8N_2$)]$_n$·$n$$H_2O$ (2): 1,10-Phenanthroline (0.40 g, 2 mmol) in ethanol (5 mL) was added dropwise with continuous stirring to an EtOH/H_2O (ca. 1:2, v/v, 20 mL) solution of maleic acid (0.34 g, 2 mmol), NaOH (0.16 g, 4 mmol), and $MnSO_4$·H_2O (0.34 g, 2 mmol). The resulting yellow solution was stirred for 10 min at room temperature, then filtered. The filtrate was left undisturbed for about one week to produce yellow crystals, which were collected and air-dried to afford **2** (0.48 g, yield 65.5% based on Mn). $C_{16}H_{12}MnN_2O_5$ (367.22): calcd. C 52.33, H 3.29, Mn 14.96, N 7.63; found C 52.56, H 3.13, Mn 15.21, N 7.41. IR: $\tilde{\nu}$ = 3450 (br), 3053 (m), 1635 (m), 1616 (s), 1558 (vs), 1516 (m), 1427 (s), 1394 (m), 1346 (m), 1306 (vs), 1200 (m), 1144 (m), 1101 (m), 991 (w), 891 (m), 866 (m), 850 (vs), 779 (m), 729 (s), 667 (w), 638 (w), 621 (m), 550 (m), 418 (m) cm^{-1}.

Synthesis of [Mn($C_4H_2O_4$)($C_{10}H_8N_2$)]$_n$ (3): The procedure used was similar to that for the preparation of **2**, except that 2,2′-bipyridine (0.31 g, 2 mmol) was used instead of 1,10-phenanthroline. Yellow crystals of **3** (0.26 g) were obtained in 40% yield. $C_{14}H_{10}MnN_2O_4$ (325.18): calcd. C 51.71, H 3.10, Mn 16.89, N 8.61; found C 51.64, H 2.98, Mn 16.97, N 8.54. IR: $\tilde{\nu}$ = 3046 (m), 1647 (w), 1595 (w), 1585 (w), 1551 (vs), 1491 (w), 1475 (m), 1429 (s), 1396 (s), 1317 (vs), 1284 (w), 1248 (w), 1217 (m), 1173 (w), 1157 (m), 1101 (w), 1059 (m), 1014 (s), 974 (m), 895 (m), 862 (m), 835 (w), 816 (w), 773 (s), 737 (m), 650 (m), 631 (m), 559 (m), 417 (m) cm^{-1}.

X-ray Crystallography: Intensity data were collected at 293 K with a Siemens SMART CCD diffractometer equipped with graphite-monochromated Mo-K_α radiation (λ = 0.71073 Å). Data were corrected for LP factors and empirical absorption correction was applied. The structures were solved by direct methods and refined on F^2 by the full-matrix, least-squares technique through use of the SHELXTL-97 program package.[19] All non-hydrogen atoms were refined anisotropically, and hydrogen atoms were introduced geometrically, with the exception of the lattice water hydrogen atoms, which were located from the difference Fourier syntheses. Crystallographic data of **1**−**3** are outlined in Table 3. CCDC- 201331 to -201333 contain the supplementary crystallographic data for complexes **1**−**3**. These data can be obtained free of charge at www.ccdc.cam.ac.uk/conts/retrieving.html [or from the Cambridge Crystallographic Data Centre, 12 Union Road, Cambridge CB2 1EZ, UK; Fax: (internat. + 44-1223/336-033; E-mail: deposit@ccdc.cam.ac.uk].

Acknowledgments

This work was supported by the NNSFC (No. 30170229), the State Key Basic Research and Development Plan of China

Table 3. Crystallographic data for **1**−**3**

	1	**2**	**3**
Empirical formula	$C_{16}H_{10}MnN_2O_4$	$C_{16}H_{12}MnN_2O_5$	$C_{14}H_{10}MnN_2O_4$
Formula mass	349.20	367.22	325.18
Space group	$P\bar{1}$	$P\bar{1}$	$P2_1/c$
a [Å]	8.2130(8)	8.1189(4)	11.4539(3)
b [Å]	8.4237(8)	9.3033(4)	13.3059(5)
c [Å]	10.5907(1)	10.5462(5)	8.8068(3)
α [°]	74.579(2)	104.65(1)	90
β [°]	84.621(2)	95.141(2)	111.429(1)
γ [°]	73.462(2)	105.327(1)	90
V [Å^3]	676.98(1)	732.76(6)	1249.41(7)
Z	2	2	4
T [°C]	20	20	20
λ(Mo-K_α) [Å]	0.71073	0.71073	0.71073
μ [mm^{-1}]	0.998	0.932	1.075
$\rho_{calcd.}$ [g cm^{-3}]	1.713	1.664	1.729
R[a]	0.0370	0.0621	0.0328
wR[b]	0.0928	0.1482	0.0856

[a] $R = \||F_o| - |F_c|\|/|F_o|$. [b] $wR = [w(|F_o| - |F_c|)^2/wF_o^2]^{1/2}$; **1**: $w = 1/[\sigma^2(F_o)^2 + (0.0577P)^2 + 0.2075P]$; **2**: $w = 1/[\sigma^2(F_o)^2 + (0.0985P)^2 + 0.0000P]$; **3**: $w = 1/[\sigma^2(F_o)^2 + (0.0520P)^2 + 0.8333P]$; $P = [(F_o)^2 + 2(F_c)^2]/3$ for all complexes.

(G1998010100), and the Expert Project of Key Basic Research of the Ministry of Science and Technology.

[1] [1a] H. O. Stump, L. Ouahab, Y. Pei, D. Gradjen, O. Kahn, *Science* **1993**, *261*, 447−449. [1b] B. Moulton, M. J. Zaworotko, *Chem. Rev.* **2001**, *101*, 1629−1658. [1c] S. Konar, P. S. Mukherjee, E. Zangrando, F. Lloret, R. N. Chaudhuri, *Angew. Chem. Int. Ed.* **2002**, *41*, 1561−1563. [1d] K. Inoue, T. Hayamizu, H. Iwamura, D. Hasaizume, Y. Ohashi, *J. Am. Chem. Soc.* **1996**, *118*, 1803−1804. [1e] F. Millange, C. Serre, G. Ferey, *Chem. Commun.* **2002**, 822−823. [1f] E. W. Lee, Y. Kim, D.-Y. Jung, *Inorg. Chem.* **2002**, *41*, 501−506. [1g] R. Robson, *J. Chem. Soc., Dalton Trans.* **2000**, 3735−3744.

[2] [2a] M. Fujita, D. Oguro, M. Milyazawa, H. Oka, K. Yamaguchi, K. Oguro, *Nature* **1995**, *378*, 469−471. [2b] D. Braga, F. Grepioni, G. R. Desiraju, *Chem. Rev.* **1998**, *98*, 1375−1405. [2c] Y.-C. Liang, R. Cao, W.-P. Su, M.-C. Hong, W.-J. Zhang, *Angew. Chem. Int. Ed.* **2000**, *39*, 3304−3307. [2d] O. M. Yaghi, H. L. Li, C. Davis, D. Richardson, T. L. D. Groy, *Acc. Chem. Res.* **1998**, *31*, 474−484.

[3] T. K. Maji, S. Sain, G. Mostafa, T.-H. Lu, J. Ribas, M. Monfort, N. R. Chaudhuri, *Inorg. Chem.* **2003**, *42*, 709−716 and references therein.

[4] [4a] J. M. Lehn, *Supramolecular Chemistry − Concepts and Perspectives*, VCH, Weinheim, **1995**. [4b]P. Losier, M. J. Zaworotko, *Angew. Chem. Int. Ed. Engl.* **1996**, *35*, 2779−2782.

[5] [5a] W.-G. Wang, C.-B. Ma, X.-F. Zhang, C.-N. Chen, Q.-T. Liu, F. Chen, D.-Z. Liao, L.-C. Li, *Bull. Chem. Soc., Jpn.* **2002**, *75*, 2609−2614. [5b] C.-B. Ma, C.-N. Chen, Q.-T. Liu, D.-Z. Liao, L.-C. Li, *Eur. J. Inorg. Chem.* **2003**, 1227−1231. [5c] C.-B. Ma, C.-N. Chen, Q.-T. Liu, D.-Z. Liao, L.-C. Li, L.-C. Sun, *New J. Chem.* **2003**, *27*, 890−894.

[6] [6a] S. S. Y. Chui, S. M. F. Lo, J. P. H. Charmant, A. G. Orpen, I. D. Williams, *Science* **1999**, *283*, 1148−1150. [6b] J. D. Dunitz, *Chem. Commun.* **2003**, 545−548.

[7] M.-X. Li, G.-Y. Xie, S.-L. Jin, Y.-D. Gu, M.-Q. Chen, J. Liu, Z. Xu, X.-Z. You, *Polyhedron* **1996**, *15*, 535−539.

[8] Z. Shi, L.-R. Zhang, S. Gao, G.-Y. Yang, J. Hua, L. Gao, S.-H. Feng, *Inorg. Chem.* **2000**, *39*, 1990−1993.

[9] C.-G. Zhang, Y.-J. Leng, Z.-F. Ma, D.-Y. Yan, *J. Chem. Crystallogr.* **1999**, *29*, 1081−1084.

[10] [10a] C.-G. Zhang, K.-B. Yu, D. Wu, C.-X. Zhao, *Acta Crystallogr., Sect. C* **1999**, *55*, 1470−1473. [10b] Y.-Q. Zheng, J. Sun, J.-L. Lin, *Z. Anorg. Allg. Chem.* **2002**, *628*, 1397−1401. [10c] C.-G. Zhang, C.-X. Zhao, Z.-F. Ma, D.-Y. Yan, *J. Coord. Chem.* **2000**, *52*, 87−92.

[11] D. N. Sathyanarayana, V. V. Savant, *Z. Anorg. Allg. Chem.* **1971**, *385*, 329−331.

[12] G. B. Deacon, R. J. Phillips, *Coord. Chem. Rev.* **1980**, *33*, 227−250.

[13] W. Hiller, J. Strahle, A. Datz, M. Hanack, W. E. Hatfield, L. W. TerHaar, P. Gutlich, *J. Am. Chem. Soc.* **1984**, *106*, 329−335.

[14] O. Kahn, *Molecular Magnetism*, VCH Publishers Inc., New York, **1993**.

[15] R. L. Carlin, *Magnetochemistry*, Springer, Berlin, Heidelberg, **1986**.

[16] [16a] Z.-N. Chen, S.-X. Liu, T. Qiu, Z.-M. Wang, J.-L. Huang, W.-X. Tang, *J. Chem. Soc., Dalton Trans.* **1994**, 2989−2993. [16b] E. Colacio, J. M. Dominguez-Vera, M. Ghazi, R. Kivekäs, M. Klinga, J. M. Moreno, *Eur. J. Inorg. Chem.* **1999**, 441−445.

[17] [17a] M. Inoue, M. Kubo, *Inorg. Chem.* **1970**, *9*, 2310−2314. [17b] R. L. Carlin, K. Kopinga, O. Kahn, M. Verdauger, *Inorg. Chem.* **1990**, *29*, 4240−4246.

[18] R. Cao, D. F. Sun, Y. C. Liang, M. C. Hong, K. Tatsumi, Q. Shi, *Inorg. Chem.* **2002**, *41*, 2087−2094.

[19] G. M. Sheldrick, *SHELXL-97*, Universität Göttingen, **1997**.

Received February 19, 2003

